



Photocatalytic Degradation of Organic Dyes Using Ag-TiO₂ Nanomaterials

KM Reddy*

Department of Chemistry, College of Engineering Studies (CoES), University of Petroleum and Energy Studies (UPES), Bidholi Campus, Dehradun, Uttarakhand, India

ABSTRACT

Photocatalytic degradation of organic dyes using Ag-TiO₂ nanomaterials, and synthesis and characterization of Ag-TiO₂ nanophotocatalysts using various instrumental techniques such as PXRD, SEM, FT-IR, UV-Visible spectrophotometer, TEM, XPS etc. The materials as prepared by sol-gel synthesis were dried in oven at 120°C followed by calcined at 450°C. Fine powdered photocatalysts were used for the photocatalysis of organic dye degradation. Organic dye which were of high risk present in water and water ponds released from various textile industries.

Keywords: Silver deposited TiO₂; Photocatalysts; NanoPhotocalysts

INTRODUCTION

Photocatalysis on semiconductor TiO₂ has been widely investigated in recent years, mainly because of its high potential for ensuring the complete destruction of organic contaminants in the aqueous medium [1-5]. Titanium dioxide is the most extensively studied photocatalytic material, with outstanding physical and chemical properties. On excitation electrons are promoted to the conduction band and holes are consequently generated in its valence band. Such charge carriers are able to reduce and oxidize many species adsorbed on the semiconductor particles and to induce the oxidative destruction of organics upto their mineralization [6-11]. The high rate of recombination between photogenerated electron-hole pairs is a major rate-determining factor controlling the photocatalytic efficiency. In this regard, noble metal deposition can improve the photocatalytic efficiency of titanium dioxide [12-16], by trapping the electrons thereby preventing the recombination. Metal islands deposited on the semiconductor surface have been shown to efficiently trap the electron and the free hole in the valence band can successively participate in the oxidation reactions [17]. The equilibration of the Fermi-level between the metal and the semiconductor favors electron accumulation in the composite metal/TiO₂ system. Kim et al., reported that silver was more effective than platinum in the plasma-driven catalyst reactor packed with TiO₂. The deposition of Ag nanoparticles on the TiO₂ titanium dioxide (TiO₂) surface was explained in the present study as a means of improving its photocatalytic activity in the degradation of MO in the aqueous phase under UV irradiation. The effect of pH on the photocatalytic activity of metallized semiconductor particles was explored.

EXPERIMENTAL SECTION

Materials

Photocatalyst TiO₂ (Reported surface area ~42 m²g⁻¹) was used as a starting material to prepare Ag-TiO₂. Silver nitrate (AgNO₃), Sodium hydroxide (NaOH) and Sulphuric acid (H₂SO₄) were obtained from Merck chemicals, Methyl Orange (MO) (Dimethyl amino-azobenzene sodium sulphonate) is obtained from Aldrich chemicals whose molecular formula is (CH₃)₂NC₆H₄NNC₆H₄SO₃Na and the formula weight is 327 and shows a λ_{max} of 469 nm. All the reagents used were of analytical grade and the solutions were prepared using double distilled water.

Analytical Instrumentations

X-ray Diffraction:

The PXRD patterns were recorded using Bruker aXS Model D8 Advanced powder X-ray diffractometer with a CuK α source ($\lambda = 1.541 \text{ \AA}$) and the scanning range employed was $2\theta = 5^\circ - 85^\circ$ at a scan rate of 2° per minute. The average crystallite size was calculated using the Scherrer's formula. The X-ray diffraction line broadening was obtained with a slow scanning speed of $1/2^\circ$ per minute. 2.2.2. Scanning Electron Microscopy (SEM) analysis and Energy Dispersive X-ray micro analysis (EDX). The particle size is obtained by SEM analysis of the samples using JEOL-JSM-6490LV scanning electron microscopy. The EDX analysis was done using Oxdord INCA 250 energy dispersive X-ray micro analyzer.

UV-Visible Absorption/Diffuse Reflectance Spectroscopy:

The absorption and diffuse reflectance spectra were recorded by using double beam UV-3101PC UV-VIS-NIR Shimadzu scanning spectrophotometer. The spectra were recorded at room temperature in the range of 200-800 nm.

FTIR Spectral Analysis:

FTIR spectra were recorded using FTIR-8400S SHIMADZU FTIR spectrophotometer, in the range of frequencies from $4000-400 \text{ cm}^{-1}$ using KBr as the reference sample.

Photocatalysis Procedure

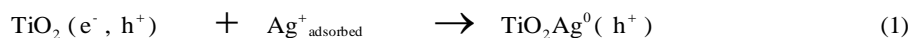
The degradation experiments were carried out in the 250 mL reactor equipped with medium pressure mercury vapour lamp with a photon flux of $7-8 \text{ mW/cm}^2$ (as determined by ferrioxalate actinometry) whose wavelength peaks around 360 nm is used. The reaction mixture stirred on magnetic stirrer with rpm 300 – 600 speed during the course of reaction at ambient temperature. 250 mL of aqueous dye solution (10 ppm) along with 20 - 50 mg of the photocatalyst ($\text{TiO}_2/\text{Ag-TiO}_2$) is irradiated with UV-light. The initial pH of the MO aqueous suspension was found to be neutral. 3 - 5 mL of sample was periodically withdrawn from the reactor and analysed after removal of TiO_2 particles by centrifugation at 3000 rpm for 15 minutes. The cleavage of the azo bond of MO leading to its bleaching was monitored by UV-Vis spectrophotometric analysis at 460 – 480 nm.

RESULTS AND DISCUSSIONS

Characterization of Photocatalysts

Silver nanoparticles are deposited on TiO_2 by photodeposition method [12]. Ag- TiO_2 photocatalyst is prepared based on the reduction of AgNO_3 in the presence of oxalic acid in TiO_2 suspension. The deposition of Ag nanoparticles on TiO_2 was confirmed by the colour change of the modified oxide powder which turns into pale pink from white, a colour derived from the surface plasmon resonance of Ag^0 islands. The absorption and diffused reflectance UV-visible spectra of TiO_2 and Ag- TiO_2 are shown in the Figures 1 and 2. The strong plasmon resonance absorption at wavelengths above 400 nm is observed due to the Ag nanoparticle deposition on TiO_2 . Light absorption by the deposited metal causes a collective oscillation of the free conduction band electrons of the silver nanoparticles as a consequence of their optical excitation. This phenomenon is observed when the wavelength of the incident light far exceeds the particle diameter.

Hermann et al [18] have proposed a mechanism describing the deposition and growth of silver particles on the titania surface. Silver ions are initially adsorbed on the surface of TiO_2 particles. Photogenerated electrons reduce adsorbed Ag^+ ions to silver metal atoms. The formation of small crystallites of silver can occur either by the agglomeration of silver atoms or by a cathodic-like successive reduction process. The agglomeration of silver atoms can be described in the following way



The successive reduction sequence is represented by



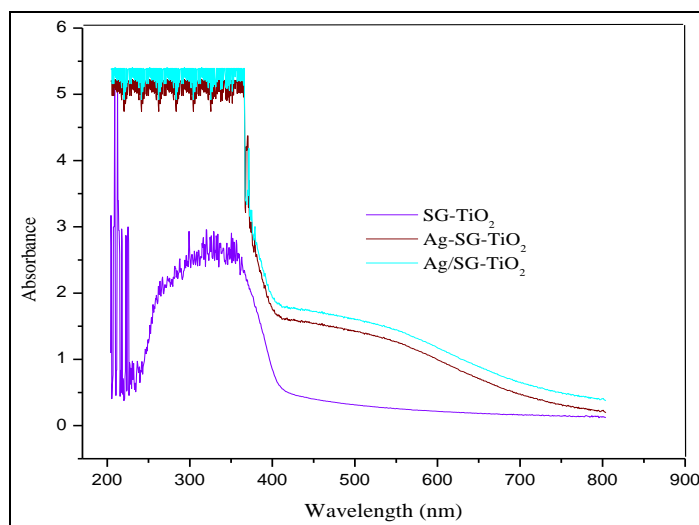


Figure 1: UV-Visible absorption spectra of (a) SG-TiO₂, Ag-SG-TiO₂, Ag/SG-TiO₂

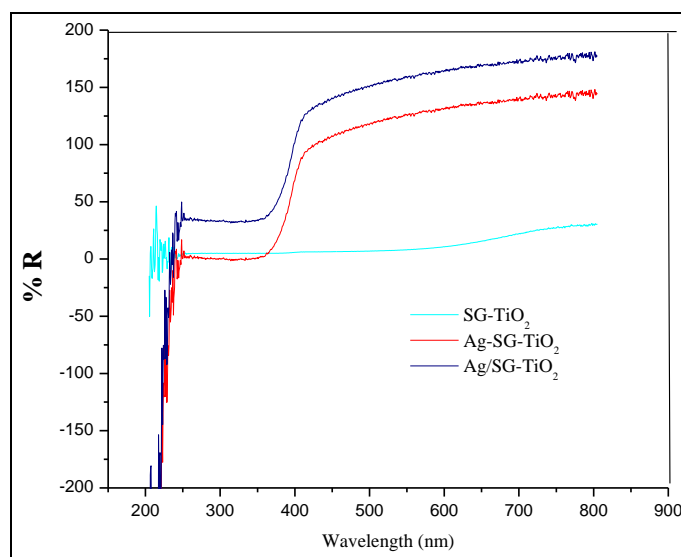


Figure 2: Diffuse Reflectance Spectra of SG-TiO₂, Ag-SG-TiO₂, Ag/SG-TiO₂

UV-Visible Absorption/Diffuse Reflectance Spectroscopy:

TiO₂ particles exhibit strong absorption band at less than 400 nm [19], which corresponds to the band gap energy (3.0 - 3.2 eV). Pure colloidal silver exhibits an absorption band at ~520 nm which is normally attributed to the typical surface plasmon absorption of silver nanoparticles. The Ag-TiO₂ semiconductor particles exhibited extended absorption ranging from 500 to 800 nm (Figures 1 and 2) in addition to the typical TiO₂ absorption profile. The reason for such a broad absorption band may be attributed to the plasmon effect shown by the silver nanoparticles.

Powdered X-ray diffraction (PXRD):

Figure 3 shows the typical PXRD patterns of pure TiO₂ and Ag-TiO₂ catalysts. The 2θ values at which major peaks appear for Ag-TiO₂ are found to be almost the same as that of pure TiO₂. This may be due to the fact that deposition does not alter the crystal structure of Ag-TiO₂. Diffractions that are attributable to anatase (A)/rutile (R) phase of TiO₂ crystals are clearly detectable at 2θ values of 25.285° (A)(3.51943)/ 27.439° (R) (3.24795) the numbers in the parenthesis represents the d-spacing values for A and R respectively. Slow scanning shows a peak at 2θ = 37.874° (Ag)(2.37360) in Ag-TiO₂, which can be assigned to (400) plane of silver which confirms the deposition of Ag on the surface of TiO₂. The anatase/ rutile lattice structure of pure TiO₂ is unperturbed in the PXRD pattern of Ag-TiO₂. The average size of Ag particles, calculated from line broadening of diffraction peak using Scherrer equation, is ~30 nm. Silver deposition did not affect the phase structure of TiO₂. Ag deposition was responsible for new peaks which

are typical of crystalline Silver 38.5° and 44° and their intensities increased with Ag loading, the Ag phase being hardly detectable in 0.23% Ag deposited Ag-TiO₂ [20].

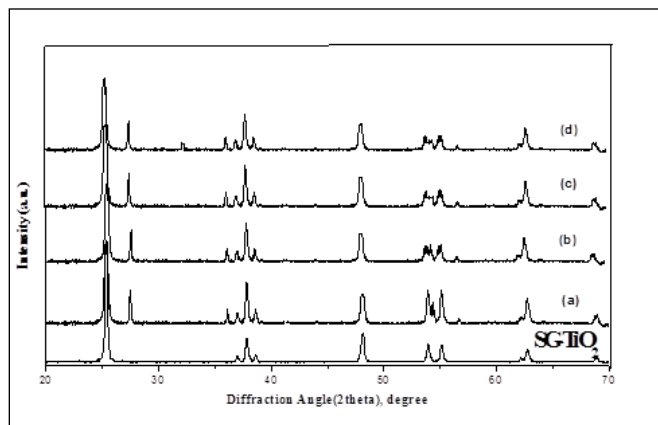


Figure 3: PXRD pattern of TiO₂ and Ag-TiO₂

SEM Analysis and Energy Dispersive X-ray Micro Analysis:

In order to investigate the morphology of the synthesized photocatalyst particles, SEM studies were performed. Figure 4 shows SEM images of the TiO₂ and Ag-TiO₂ particles at two different magnifications. The images illustrate that the particles are spherical and have a smooth surface in Ag-TiO₂. This conventional photodeposition method leads to heterocoagulation where the nanosized Ag deposits are formed on the surface of TiO₂ spheres. The surface composition of Ag-TiO₂ was qualitatively determined by EDX analysis. It showed that weight (%) and atomic (%) concentrations ratios of Ti plus O to Ag as 16.7/0.14 and 99.77/ 0.23, respectively (Figure 5 and Table 1).

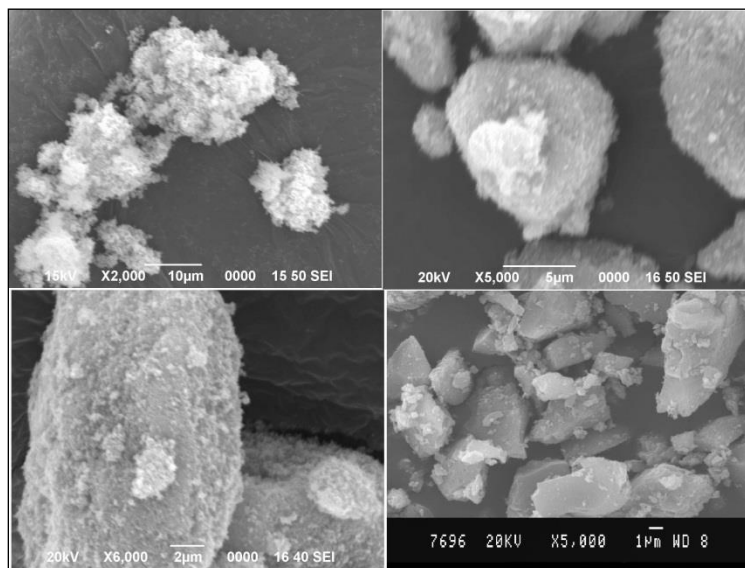


Figure 4: SEM images with surface morphologies of TiO₂ and Ag-TiO₂

FTIR Spectral Analysis:

The Infrared spectra of TiO₂ and Ag-TiO₂ powders in the range 4000-400 cm⁻¹ shows a broad band at 3400 cm⁻¹ which can be assigned to γ_{OH} stretching mode of O-H vibration of the Ti-OH [21]. The other narrow band at 1640 cm⁻¹ can be assigned either to δ_{OH} bending modes of hydroxyl group or to the stretching mode of Ti-O (γ_{Ti-O}) which could be the envelope of the bands of Ti-O-Ti bond of a titanium oxide network. This band increases in its intensity for Ag-TiO₂ suggesting the surface to be more hydroxylated compared to TiO₂.

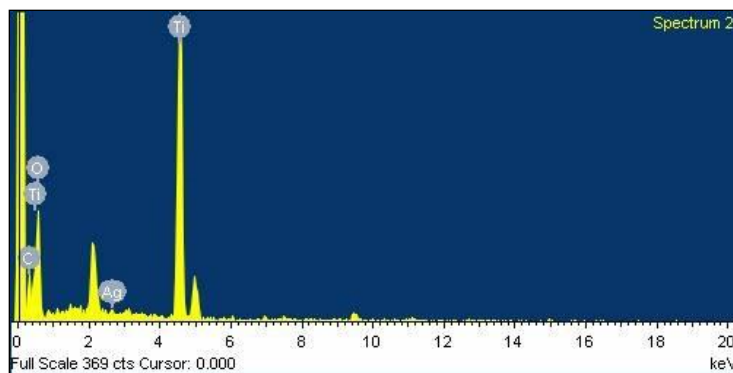
Figure 5: EDAX spectrum of Ag-TiO₂ sample

Table 1: EDX analysis %

Element Compound %	Element %	Atom %
Ti	59.95	33.25
O	40.05	66.75
Total	100	100

Photocatalytic Activity

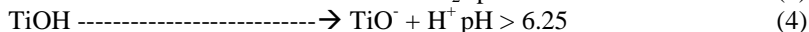
Preliminary tests, performed to verify the adsorption properties of photocatalysts show that the adsorption was high on Ag-TiO₂. The extent of adsorption of MO was determined, after continuous stirring for one hour in the dark at laboratory temperature using the formula $Q = (C_0 - C_e) V/W$, where Q is the extent of adsorption, C₀ and C_e are concentrations before and after adsorption, V is the volume of the reaction mixture and W is amount of catalyst added. The value of Q is found to be 5.123×10^{-3} ppm mL mg⁻¹ [22].

The iso-electric point of Ag-TiO₂ has been reported to shift to lower pH values with respect to unmodified TiO₂, thus, extending the pH region where the photocatalyst surface is negatively charged. This inhibits the adsorption of negatively charged dye radicals such as the bisulphonic azo dye MO. The first order kinetic rate constant for the photocatalytic degradation of MO photomineralisation profile with TiO₂ and Ag-TiO₂ suspensions and is monitored by UV-Visible spectral analysis..

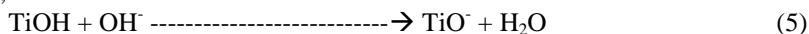
Effect of pH

The effect of pH on the rate of azo dye photodegradation was investigated in the presence of TiO₂ and Ag-TiO₂. The results obtained in the pH range 3-9, which shows that the enhanced photodegradation was obtained at neutral pH for both the catalysts. Azo dye such as MO is red coloured below pH 3 and appears yellow above 4.5 (pK_{in} ≈ 3.7) and the colour depends upon the concentration of H⁺ and OH⁻ ions. Further the capacity of adsorption on TiO₂ and Ag-TiO₂ at different pH values can be explained by the intrinsic amphoteric behaviour (Ti-OH) of suspended catalyst particles and the acidic/basic nature of the dye molecule. This photocatalyst surface have active role in the photodegradation reaction.

In acidic solution, the possible reactions are



In alkaline solutions,



CONCLUSION

High photocatalytic activity due to the electron trapping by the silver metal deposit, higher extent of light absorption and degree of hydroxylated surface will enhance the photocatalytic reaction in Ag deposited TiO₂ nanophotocatalysts. The degradation is most efficient at neutral pH for the catalysts. Photocatalytic degradation of organic dyes using Ag-TiO₂ nanomaterials, and synthesis and characterization of Ag-TiO₂ nanophotocatalysts using various instrumental techniques such as PXRD, SEM, FT_IR, UV-Visible spectrophotometer, TEM, XPS results were illustrate the better catalysis. The materials as prepared by sol-gel synthesis were dried in oven at 120°C followed by calcined at 450°C. Fine powdered photocatalysts were used for the photocatalysis of organic dye degradation. Organic dye which were of high risk present in water and water ponds released from various textile industries.

ACKNOWLEDGMENTS

Author is grateful for kind support of UPES, Dehradun and BUB, Bangalore for collaborations.

REFERENCES

- [1] M Schiavello. Photocatalysis and Environment. Trends and Applications, Kluwer Academic Publishers, Dordrecht, **1988**.
- [2] E Pelizzetti, N Serpone. Photocatalysis. Fundamentals and Applications, Wiley, New York, **1989**.
- [3] MR Hoffmann; SC Martin; W Choi; DW Behnemann. *Chem Rev* **1995**, 95, 69-96.
- [4] A Hogfelt; M Gretzel. *Chem Rev.* **1995** 95, 49-68.
- [5] JM Herrman; H Tahiri; Y Ait-Ichou; G Lassaletta; AR Gonzalaz-Elipe; A Fernandez. *Appl Catal B Environ.* **1997**, 13, 219-228.
- [6] MA Fox; MT Dulay. *Chem Rev.* **1993**, 93, 341-357.
- [7] A Heller. *Acc Chem Rev.* **1995**, 28, 503-508.
- [8] M Anpo, H Yamashita. In: Surface Photochemistry, Wiley, Chichester, **1996**, 117-164.
- [9] PV Kamat. *Chem Rev.* **1993**, 93, 267-300.
- [10] DM Blake; PC Maness; Z Huang; EJ Wolfrum; J Huang; WA Jacoby. *Sep Purif Method.* **1999**, 28, 1-50
- [11] A Agostiano; A Albini; F Bordin; JP Fouassier; MP Gordon; H Lemmetyinen; UE Steiner; T Yagishita. *Trend Photochem Photobiol.* **1997**, 4, 79-86.
- [12] E Szabo-Bardos; H Czili; A Horvath. *J Photochem Photobiol A Chem.* **2003**, 154, 195-201.
- [13] E Szabo-Bardos; H Czili; A Horvath. *J Photochem Photobiol A Chem.* **2006**, 184, 221-227.
- [14] WD Kingery, HK Bowen, DR Ulmann. Introduction to ceramics, Wiley-Interscience, New York, NY, **1976**, 457.
- [15] A Sarkany; Z Revay. *Appl Catal A Gen.* **2003**, 243, 347-355.
- [16] HH Kim; SM Oh; A Ogata; S Futamura. *Appl Catal B Environ.* **2005**, 56, 213-220.
- [17] FB Li; XZ Li. *Chemosphere.* **2002**, 48, 1103-1111.
- [18] JM Hermann; A Sclafani. *J Photochem Photobiol A Chem.* **1998**, 113, 181-188.
- [19] D Duonghong; E Borgarello; M Gretzel. *J Am Chem Soc.* **1981**, 103, 4685-4690.
- [20] M Mrowetz; E Selli. *J Photochem Photobiol A Chem.* **2006**, 180, 15-22.
- [21] JM Hermann; J Disdier; MN Mozzanega; P Pichat. *J Catal.* **1979**, 60, 369-377.
- [22] P Pichat; J Disdier; JM Hermann; P Vaudano. *Nouy J Chim.* **1986**, 10, 545-551.